Energy Spectrum of Two-Dimensional Excitons in a Nonuniform Dielectric Medium

M. R. Molas,[1,2,*] A. O. Slobodeniuk,[1] K. Nogajewski,[1,2] M. Bartos,[1,3] Ł. Bala,[1,2] A. Babiński,[2] K. Watanabe,[4] T. Taniguchi,[4] C. Faugeras,[1] and M. Potemski[1,2,†]

[1]*Laboratoire National des Champs Magnétiques Intenses, CNRS-UGA-UPS-INSA-EMFL,
25 avenue des Martyrs, 38042 Grenoble, France*
[2]*Institute of Experimental Physics, Faculty of Physics, University of Warsaw, ul. Pasteura 5, 02-093 Warszawa, Poland*
[3]*Central European Institute of Technology, Brno University of Technology, Purkyňova 656/123, 61200 Brno, Czech Republic*
[4]*National Institute for Materials Science, 1-1 Namiki, Tsukuba 305-0044, Japan*

We demonstrate that, in monolayers (MLs) of semiconducting transition metal dichalcogenides, the s-type Rydberg series of excitonic states follows a simple energy ladder: $\epsilon_n = -\mathrm{Ry}^*/(n + \delta)^2$, $n = 1, 2, \ldots$, in which Ry^* is very close to the Rydberg energy scaled by the dielectric constant of the medium surrounding the ML and by the reduced effective electron-hole mass, whereas the ML polarizability is accounted for only by δ. This is justified by the analysis of experimental data on excitonic resonances, as extracted from magneto-optical measurements of a high-quality WSe$_2$ ML encapsulated in hexagonal boron nitride (hBN), and well reproduced with an analytically solvable Schrödinger equation when approximating the electron-hole potential in the form of a modified Kratzer potential. Applying our convention to other MoSe$_2$, WS$_2$, MoS$_2$ MLs encapsulated in hBN, we estimate an apparent magnitude of δ for each of the studied structures. Intriguingly, δ is found to be close to zero for WSe$_2$ as well as for MoS$_2$ monolayers, what implies that the energy ladder of excitonic states in these two-dimensional structures resembles that of Rydberg states of a three-dimensional hydrogen atom.

Coulomb interaction in a nonuniform dielectric medium [1,2] is one of the central points in investigations of large classes of nanoscale materials, such as graphene [3,4], colloidal nanoplatelets [5], two-dimensional (2D) perovskites [6,7], and other atomically thin crystals including their heterostructures [8]. This problem has been largely discussed in reference to investigations of excitons in monolayers (MLs) of semiconducting transition metal dichalcogenides (S-TMDs) [9–13]. Surprisingly, at first sight, the Rydberg series of s-type excitonic states in these 2D semiconductors does not follow the model system of a 2D hydrogen atom [14–16], with its characteristic energy sequence, $\sim 1/(n - 1/2)^2$, of states with a principal quantum number n. The main reason for that is a dielectric inhomogeneity of the 2D S-TMD structures, i.e., MLs surrounded by alien dielectrics. At large electron-hole (e-h) distances, the Coulomb interaction scales with the dielectric response of the surrounding medium, whereas it appears to be significantly weakened at short e-h distances by the usually stronger dielectric screening in the 2D plane. A common approach to account for the excitonic spectra of S-TMD MLs refers to the numerical solutions of the Schrödinger equation, in which the e-h attraction is approximated by the Rytova-Keldysh (RK) potential [1,2]. However, it is only solvable numerically. A more phenomenological and intuitive approach, presented below, might be an optional solution to this problem.

In this Letter, we demonstrate that the energy spectrum, ϵ_n ($n = 1, 2, \ldots$), of Rydberg series of s-type excitonic states in S-TMD MLs may follow an energy ladder: $\epsilon_n = -\mathrm{Ry}^*/(n + \delta)^2$. From magneto-optical investigations, we accurately establish that $\mathrm{Ry}^* = 140.5$ meV and $\delta = -0.083$ for a WSe$_2$ ML encapsulated in hexagonal boron nitride (hBN). The $\epsilon_n = -\mathrm{Ry}^*/(n + \delta)^2$ ansatz is well reproduced with an analytical approach in which the e-h potential is assumed to have the form of a modified Kratzer potential [17]. Here $\mathrm{Ry}^* = \mathrm{Ry}(\mu/\varepsilon^2 m_0)$ is the effective Rydberg energy, scaled by the dielectric constant ε of the surrounding hBN medium and the reduced e-h mass μ, where $\mathrm{Ry} = 13.6$ eV and m_0 is the free electron mass. Dispersion of the Ry^* and δ parameters in different studied samples, WSe$_2$, MoSe$_2$, MoS$_2$, and WS$_2$ MLs encapsulated in hBN, is discussed, and the reduced e-h masses in these ML structures are estimated.

To accurately determine the characteristic ladder of s-type excitonic resonances in the experiment, we profited from a particularly suitable for this purpose method of magneto-optical spectroscopy [18,19]. The active part of the structure used for these experiments was a WSe$_2$ ML embedded between hBN layers. More details on the samples preparation and the experimental techniques can be found in the Supplemental Material (SM) [20]. We measured the (circular) polarization resolved magneto-photoluminescence (magneto-PL) at low temperatures
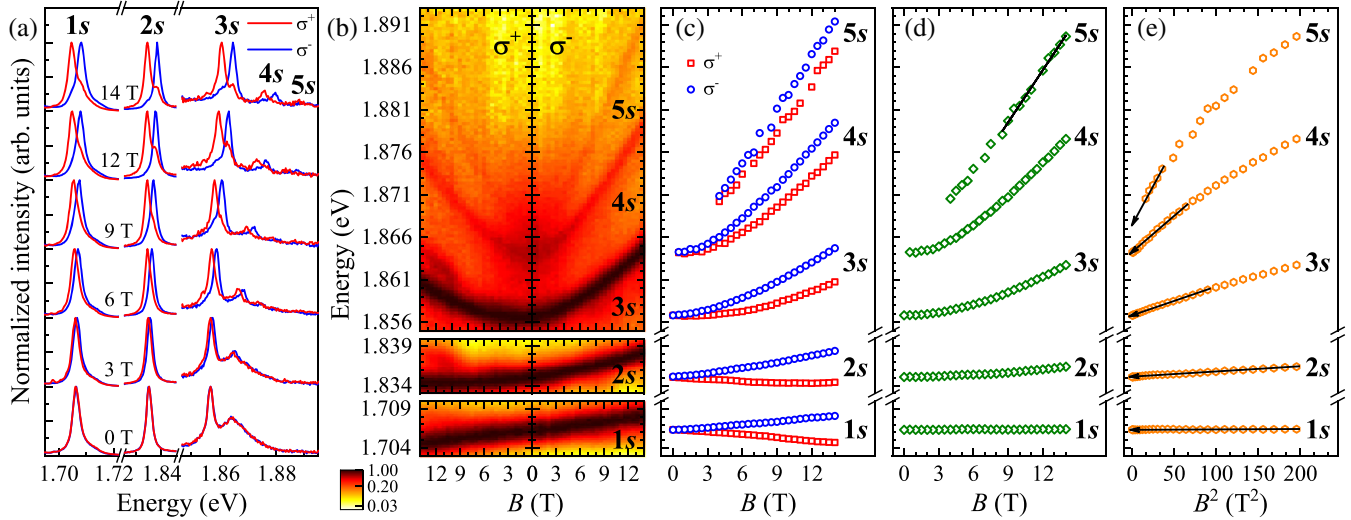
FIG. 1. (a) Helicity-resolved ($\sigma^{\pm}$) PL spectra of WSe$_2$ ML at selected magnetic fields. The separate parts of the spectra are normalized to the intensity of the $1s$, $2s$, and $3s$ lines. (b) False-color map of the corresponding PL spectra from 0 to 14 T. (c) Obtained excitonic energies for $\sigma^{\pm}$ components as a function of the magnetic field. Mean energies of the $\sigma^{\pm}$ components of excitonic resonances measured on WSe$_2$ ML as a function of (d) B and (e) B^2. The black lines are obtained by fitting the presented data with (d) $E_{5s}(B) = A + 9/2\hbar\omega_c^*$ (A is a fitting parameter) and (e) $E_{ns}(B) = E_{ns}(B=0) + \sigma B^2$.

(4.2 K) and in magnetic fields up to 14 T, applied in the direction perpendicular to the monolayer plane. Here we focus on the magneto-PL spectra of our WSe$_2$ ML, observed in the spectral range from ~1.7 to ~1.9 eV. As shown in Figs. 1(a) and 1(b), these spectra are composed of up to five PL peaks, which are clearly resolved in the range of high magnetic fields. Following a number of previous investigations [24,38–41] on similar structures, the observed PL peaks are identified with a series of excitonic resonances forming the $1s, 2s, …, 5s$ Rydberg series of the so-called A exciton [11,12]. Each ns PL peak demonstrates the Zeeman effect. This is illustrated in Fig. 1(c), in which the energies of the $\sigma^{\pm}$-polarized PL peaks are plotted as a function of the magnetic field. In accordance with previous reports, we extract $g = -4.1$ for the g factor of the $1s$ resonance but read a significantly stronger Zeeman effect for all excited states ($g \sim -4.8$). The later observation is intriguing and should be investigated in more detail, which is, however, beyond the scope of this Letter. We have also carried out magneto-PL experiments on MoS$_2$ and WS$_2$ monolayers encapsulated in hBN, but only the $1s$ and $2s$ resonances could be observed in these structures in the range of magnetic fields applied (see the SM for details).

The magnetic field evolution of the mean energies of $\sigma^{\pm}$ PL peaks is illustrated in Figs. 1(d) and 1(e). These energies, E_{ns}, are plotted as functions of the magnetic field B in Fig. 1(d), and its square B^2 in Fig. 1(e), which illustrate the characteristic behavior of ns states in the low- and high-field regime [14,19]. The high-field limit for a given ns resonance appears when $l_B \ll r_{ns}$, $E_b^{ns} \ll \hbar\omega_c^*/2$. Here r_{ns} and E_b^{ns} denote the root-mean-square radius and the binding energy $E_b^{ns} = E_g - E_{ns}$ of a given ns state at $B = 0$, $\hbar\omega_c^* = \hbar eB/\mu$,

$l_B = \sqrt{\hbar/eB}$ is the magnetic length, and other symbols have their conventional meaning. In the high-field limit, the energies of E_{ns} resonances approach a linear dependence upon B, with a slope given by $(n - 1/2)\hbar\omega_c^*$. In the low-field limit ($l_B \gg r_{ns}$, $E_b^{ns} \gg \hbar\omega_c^*/2$), the ns resonances display the diamagnetic shifts: $E_{ns}(B) = E_{ns}(B=0) + \sigma B^2$, with the diamagnetic coefficients $\sigma = (er_{ns})^2/8\mu$. The $1s$ and $2s$ resonances follow the low-field regime in the entire range of the magnetic fields investigated due to their small exciton's radii and/or large binding energies; see Fig. 1(e). The high-field regime is approached for the $5s$ resonances with an approximate linear dependence of E_{5s} with B, in the range above ~8 T. This dependence, marked with a solid line in Fig. 1(d), displays a slope of 2.1 meV/T, which, if compared to $(9/2)\hbar\omega_c^*$ dependence, provides an estimate of 0.25 m_0 for the reduced mass in the WSe$_2$ ML. However, one may also argue that working with magnetic fields up to 14 T only, the high-field limit is still barely developed even for the $5s$ state. In this context, our estimation of the reduced effective mass should be seen as its upper bound and, in the following we assume $\mu = 0.2\ m_0$ for the WSe$_2$ ML, following the results of experiments performed in fields up to 60 T [24].

In the following, we focus on the energy sequence E_{ns} of $1s, 2s, …, 5s$ excitonic resonances as they appear in the absence of a magnetic field. As shown in Fig. 1(e), the E_{ns} values are determined with linear extrapolations of E_{ns} versus B^2 dependences to $B = 0$. Next, we assume that the sequence E_{ns} obeys the rule
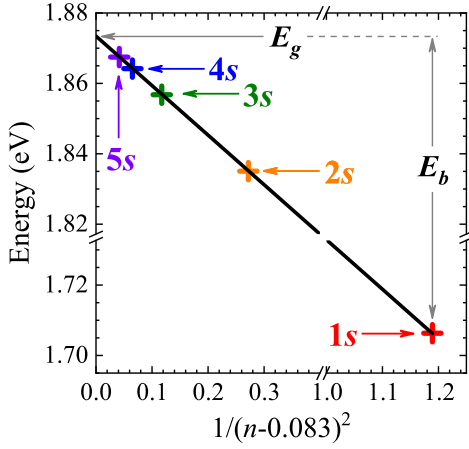
$$E_{ns} = E_g - Ry^*/(n + \delta)^2, \tag{1}$$

FIG. 2. Experimentally obtained transition energies for the exciton states as a function $1/(n+\delta)^2$ for $\delta = -0.083$. The black line shows a fit of the data to the model described by Eq. (1). The gray lines denote the band gap (E_g) and excitonic binding (E_b) energies.
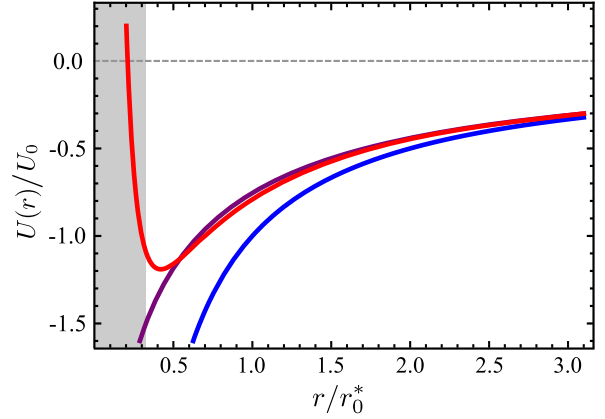

FIG. 3. Rytova-Keldysh (purple curve), Coulomb (blue curve), and Kratzer potential with $g^2 = 0.21$ (red curve), as a function of dimensionless parameter r/r_0^*. The energy scale is measured in units of $U_0 = e^2/r_0$. The gray rectangular depicts the region of distances smaller than the lattice constant $a = 3.28$ Å of WSe$_2$ MLs encapsulated in hBN ($r_0^* = 10$ Å).

where, at this point, E_g, Ry*, and δ are regarded as adjustable parameters. To test the above formula against the experimental data, we note that Eq. (1) implies that the ratio $(E_{3s} - E_{1s})/(E_{2s} - E_{1s})$ depends only on δ, and, reading it from the experiment, we extract $\delta = -0.083$. With this value, we find (see Fig. 2) that our experimental E_{ns} series perfectly matches Eq. (1) together with $E_g = 1.873$ eV and Ry$^* = 140.5$ meV (or exciton binding energy $E_b = E_g - E_{1s} = 167$ meV). The above E_g and E_b values are in very good agreement with those already reported in the literature [24]. Relevant for our further analysis is the observation that the derived value for Ry* coincides well with the effective Rydberg energy Ry$^* = 13.6$ eV $\times \mu/(\varepsilon^2 m_0) = 134.3$ meV, scaled by the dielectric constant of the surrounding hBN material $\varepsilon = \varepsilon_{hBN} = 4.5$ [27] and the reduced effective mass $\mu = 0.2m_0$ [24] of the WSe$_2$ ML. Intriguingly, the extracted δ parameter is close to zero, which implies that the $\epsilon_n = E_{ns} - E_g$ Rydberg series found in a 2D system resembles that of a 3D hydrogen atom ($\epsilon_n \sim -1/n^2$).

On the theoretical ground, the problem of excitonic spectrum in S-TMD MLs is commonly solved by invoking the Rytova-Keldysh potential [1,2] $U_{RK}(r)$ (the purple curve in Fig. 3) to account for a specific character of the e-h attraction in these systems. At large e-h distances r, $U_{RK}(r)$ coincides with a usual Coulomb potential $U_{RK}(r) \sim -e^2/\varepsilon r$ (the blue curve in Fig. 3), which scales with the dielectric constant ε of the material surrounding the monolayer. On the other hand, $U_{RK}(r) \sim \log(r\varepsilon/r_0)$ when r is small, which accounts for the effective dielectric screening length $r_0 = 2\pi\chi_{2D}$ in the system, where χ_{2D} is the 2D polarizability of the S-TMD ML. Distinctly, the apparent excitonic spectra and the related exciton binding energies critically depend on the efficiency of dielectric

screening of the electron-hole attraction in the medium surrounding the monolayer.

Whereas previous efforts have been largely focused on the numerical study of such a problem, we show that our model provides the analytical solution, which is in good agreement with the experimental results discussed above. We propose replacing $U_{RK}(r)$ with the approximate potential $U_{app}(r)$, taken in the form of piecewise function. Namely, the subfunction $U_{cor}(r)$ defines $U_{app}(r)$ at small distances r (the core domain), while the external potential $U_{ext}(r)$ corresponds to $U_{app}(r)$ in the region outside of the core.

We choose the external potential in the form of the modified Kratzer potential [17] (given in cgs units)

$$U_{ext}(r) = -\frac{e^2}{r_0}\left(\frac{r_0^*}{r} - \frac{g^2 r_0^{*2}}{r^2}\right), \quad (2)$$

where $r_0^* = r_0/\varepsilon$ is the reduced screening length and g is a tunable parameter. For the case of $g^2 = 0.21$, $U_{ext}(r)$ fits $U_{RK}(r)$ in the region $r > r_{min} = 0.46r_0^*$, with the relative deviation less than 5%. For the WSe$_2$ ML encapsulated in hBN, the distance $r_{min} = 4.6$ Å is comparable with the lattice constant $a = 3.28$ Å [42] of WSe$_2$ (see Fig. 3 for a comparison).

The Schrödinger equation with the Kratzer potential (2) provides the excitonic spectrum of the s-type states (see the SM for details)

$$\epsilon_n = -\text{Ry}^*/(n + g\kappa - 1/2)^2, \quad (3)$$

in which $\kappa^2 = 2r_0^*/a_B^*$ and $a_B^* = \hbar^2\varepsilon/\mu e^2$ is the effective Bohr radius. The effective Rydberg constant Ry$^* = e^2/2\varepsilon a_B^*$

sets the energy scale in the system, while $\delta = g\kappa - 1/2$ defines the relative positions of the energy levels in the spectrum. Note that Eq. (3) is analogous to our experimentally found relation given by Eq. (1).

In the following, we introduce $U_{\text{cor}}(r)$, which replaces the Kratzer potential at small distances r, comparable to the lattice constant of WSe$_2$. We choose the constant attractive potential $U_{\text{cor}}(r) = V_0$. Below we demonstrate that it does not change the $\propto (n + \delta)^{-2}$ behavior of the spectrum and modifies only the δ parameter.

We consider the Kratzer and constant potentials as external and core ones, respectively. We choose the parameter $g^2 = 0.21$ and the region of validity of the Kratzer potential up to its minimum $\xi_0 = 2g^2$, where $\xi = r/r_0^*$. The parameter V_0 of the core potential is chosen as an average value of $U_{\text{RK}}(\xi)$ in the domain $\xi \in [0, \xi_0]$: $V_0 = 2\xi_0^{-2} \int_0^{\xi_0} d\xi \xi U_{\text{RK}}(\xi)$. Finally the approximate potential is

$$U_{\text{app}}(\xi) = -U_0 \left\{ \left[\frac{1}{\xi} - \frac{0.21}{\xi^2} \right] \theta(\xi - \xi_0) + v_0 \theta(\xi_0 - \xi) \right\}, \quad (4)$$

where $\theta(x)$ is the step function and $v_0 = 1.711\,34$. Note that the truncated Kratzer potential is applicable only if the radius of the core potential r_{cor} is less than or comparable to the lattice constant a. We estimate that this requirement is well satisfied for all monolayers encapsulated in hBN, and in particular for our WSe$_2$ structure. Considering the s-type excitonic states in this later system, we derive the following formula (a detailed description is given in the SM):

$$\epsilon_n = -134 \text{ meV}/(n - 0.099)^2. \quad (5)$$

Both found values, 134 meV and -0.099, match their experimentally obtained counterparts [with the aid of Eq. (1)] Ry$^* = 140.5$ meV and $\delta = -0.083$.

The applicability range of the formula given by Eq. (1) can also be considered from a different angle, i.e., when it is directly compared or fitted to numerical solutions obtained within the Rytova-Keldysh formalism. As demonstrated in the SM, the validity range of Eq. (1) can be defined with respect to a single, dimensionless parameter of a monolayer structure, $b = a_B^*/r_0^*$, and we find that our simple approach is valid when $b > 0.3$ and estimate that this condition is well satisfied for all monolayers encapsulated in hBN. Nevertheless, even if b is as small as $b \approx 0.1$, which may correspond to the case of a monolayer deposited on a Si/SiO$_2$ substrate, the spectrum given by Eq. (1) coincides with that derived with the Rytova-Keldysh potential within an accuracy of 5%.

The model proposed above accounts well for the experimental results obtained for the WSe$_2$ monolayer, and it would be interesting to test this model for other S-TMD materials. Unfortunately, the observation of the rich Rydberg spectrum of excitonic states in S-TMD MLs
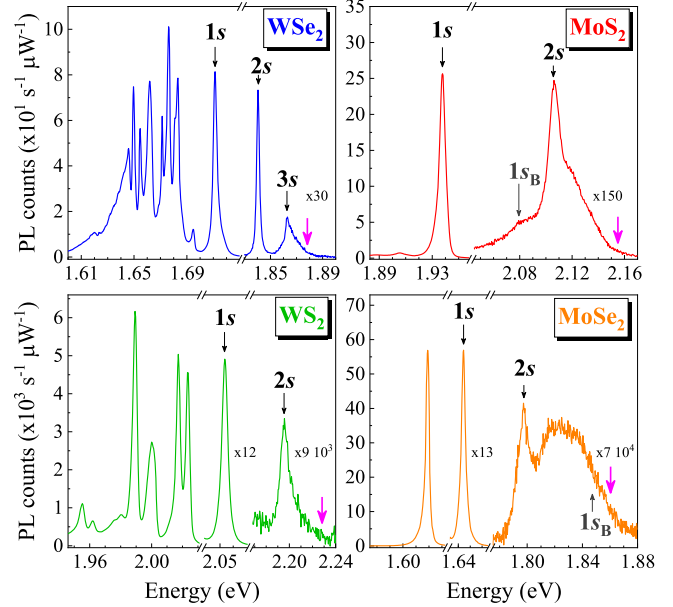

FIG. 4. Low temperature PL spectra of S-TMD MLs at $T = 5$ K. The pink vertical arrows denote the estimated bandgap energies E_g. The chosen spectral regions are scaled for clarity. Typically for S-TMDs monolayers, the most pronounced emission feature seen in our spectra is due to the $1s$ excitonic resonance accompanied by low energy peaks commonly assigned to different excitonic complexes [33,40,43–53].

seems to be, so far, uniquely reserved for WSe$_2$ MLs. Nevertheless, for all other S-TMD MLs studied, i.e., MoS$_2$, WS$_2$, and MoSe$_2$ MLs encapsulated in hBN, we observe the $2s$ in addition to the $1s$ excitonic resonance; see Fig. 4 and Fig. S7 in the SM. The energy positions, E_{1s} and E_{2s}, of the $1s$ and $2s$ resonances (of the A exciton) are directly read from Fig. 4. Of interest is the energy difference $(E_{2s} - E_{1s}) = \Delta E_{2s-1s}^{\text{exp}}$, listed in Table I for all four MLs investigated.

As shown in Fig. 4, the PL peaks associated with the excited excitonic states are followed by noticeable PL tails developed at higher energies. We believe that these tails penetrate above the band-gap energies, which are, however, not spectacularly marked in the spectra. We note that in the case of our WSe$_2$ ML, the PL intensity at the band-gap energy (accurately estimated from magneto-PL data and marked with a pink arrow in Fig. 4) consists of 5% of the intensity of the $2s$ exciton PL peak. Applying the same convention to all spectra presented in Fig. 4, we estimate the band gaps in the three other MLs, as illustrated with pink arrows in the figure. Most critical is an estimation of the band gap in MoSe$_2$ ML (see the SM for details). With the estimation of the band gap and reading the energies of $1s$ excitonic resonances directly from the spectra (see Fig. 4), we extract exciton binding energies $E_b^{\text{exp}} = (E_g - E_{1s})$ and show their values in Table I. Having estimated the $\Delta E_{2s-1s}^{\text{exp}}$ and E_b^{exp} parameters, and following

TABLE I. Series of parameters (E_b^{exp}, $\Delta E_{2s-1s}^{\mathrm{exp}}$, δ^{exp}, μ^{exp}) obtained from the analysis of PL spectra shown in Fig. 4 compared with results of density-functional theory (DFT) calculations (μ^{DFT}) [42].

Monolayer	E_b^{exp} (meV)	$\Delta E_{2s-1s}^{\mathrm{exp}}$ (meV)	δ^{exp}	μ^{exp} (m_0)	μ^{DFT} (m_0)
WSe$_2$	167	130	-0.083	0.21	0.16
MoSe$_2$	216	153	0.174	0.44	0.27
WS$_2$	174	141	-0.229	0.15	0.15
MoS$_2$	217	168	-0.095	0.26	0.24

our predictions that $E_{ns} = E_g - \mathrm{Ry}^*/(n+\delta)^2$, where $\mathrm{Ry}^* = \mathrm{Ry} \times \mu/(\varepsilon_{\mathrm{hBN}}^2 m_0)$, we derive the δ^{exp} and μ^{exp} parameters for all MLs studied; see Table I. We found very good agreement between our estimations and the results of DFT calculations [42] for the reduced masses in WS$_2$ and MoS$_2$ MLs, while we note an apparent discrepancy for WSe$_2$ and MoSe$_2$ MLs. We also applied our model to estimate values of band gaps and binding energies to the experimental data available in the literature [9,37], which is discussed in the SM.

Concluding, we have demonstrated that the ns Rydberg series of excitonic states in S-TMD monolayers encapsulated in hBN follows a simple energy ladder: $\epsilon_n = -\mathrm{Ry}^*/(n+\delta)^2$. $\mathrm{Ry}^* = \mathrm{Ry} \times \mu/(\varepsilon^2 m_0)$, where Ry is the Rydberg energy, μ denotes the reduced e-h mass, and ε is the dielectric constant of the surrounding material. The dielectric polarizability χ_{2D} of a monolayer is encoded only in δ. Strikingly, δ is found to be close to zero for a WSe$_2$ (and MoS$_2$) ML whose ϵ_n spectrum resembles that of a 3D hydrogen atom. The proposed model may be applicable to other Coulomb bound states (e.g., donor and/or acceptor states), and also to other systems, such as colloidal platelets [5] and 2D perovskites [6]. Interestingly, the $\epsilon_n = -\mathrm{Ry}^*/(n+\delta)^2$ formula coincides with that expected for a hypothetical hydrogen atom in fractional dimension N, ($N = 2\delta + 3$), which was indeed speculated [16] to mimic the spectrum of Coulomb bound states in low-dimensional semiconductor structures.

*maciej.molas@fuw.edu.pl
†marek.potemski@lncmi.cnrs.fr

[1] N. S. Rytova, Phys. Astron. **3**, 308 (1967).
[2] L. V. Keldysh, JETP Lett. **29**, 658 (1979).
[3] V. N. Kotov, B. Uchoa, V. M. Pereira, F. Guinea, and A. H. Castro Neto, Rev. Mod. Phys. **84**, 1067 (2012).
[4] C. Faugeras, S. Berciaud, P. Leszczynski, Y. Henni, K. Nogajewski, M. Orlita, T. Taniguchi, K. Watanabe, C. Forsythe, P. Kim, R. Jalil, A. K. Geim, D. M. Basko, and M. Potemski, Phys. Rev. Lett. **114**, 126804 (2015).
[5] S. Ithurria, M. D. Tessier, B. Mahler, R. P. S. M. Lobo, and B. Dubertret, and Al. L. Efros, Nat. Mater. **10**, 936 (2011).
[6] C. C. Stoumpos, D. H. Cao, D. J. Clark, J. Young, J. M. Rondinelli, J. I. Jang, J. T. Hupp, and M. G. Kanatzidis, Chem. Mater. **28**, 2852 (2016).
[7] J.-C. Blancon, A. V. Stier, H. Tsai, W. Nie, C. C. Stoumpos, B. Traoré, L. Pedesseau, M. Kepenekian, F. Katsutani, G. T. Noe, J. Kono, S. Tretiak, S. A. Crooker, C. Katan, M. G. Kanatzidis, J. J. Crochet, J. Even, and A. D. Mohite, Nat. Commun. **9**, 2254 (2018).
[8] A. K. Geim and I. Grigorieva, Nature (London) **499**, 419 (2013).
[9] A. Chernikov, T. C. Berkelbach, H. M. Hill, A. Rigosi, Y. Li, O. B. Aslan, D. R. Reichman, M. S. Hybertsen, and T. F. Heinz, Phys. Rev. Lett. **113**, 076802 (2014).
[10] A. Raja, A. Chaves, J. Yu, G. Arefe, H. M. Hill, A. F. Rigosi, T. C. Berkelbach, P. Nagler, C. Schüller, T. Korn, C. Nuckolls, J. Hone, L. E. Brus, T. F. Heinz, D. R. Reichman, and A. Chernikov, Nat. Commun. **8**, 15251 (2017).
[11] M. Koperski, M. R. Molas, A. Arora, K. Nogajewski, A. Slobodeniuk, C. Faugeras, and M. Potemski, Nanophotonics **6**, 1289 (2017).
[12] G. Wang, A. Chernikov, M. M. Glazov, T. F. Heinz, X. Marie, T. Amand, and B. Urbaszek, Rev. Mod. Phys. **90**, 021001 (2018).
[13] M. Trushin, M. O. Goerbig, and W. Belzig, Phys. Rev. Lett. **120**, 187401 (2018).
[14] A. H. MacDonald and D. S. Ritchie, Phys. Rev. B **33**, 8336 (1986).
[15] E. S. Koteles and J. Y. Chi, Phys. Rev. B **37**, 6332 (1988).
[16] P. Christol, P. Lefebvre, and H. Mathieu, J. Appl. Phys. **74**, 5626 (1993).
[17] A. Kratzer, Z. Phys. **3**, 289 (1920).
[18] O. Akimoto and H. Hasegawa, J. Phys. Soc. Jpn. **22**, 181 (1967).
[19] M. Potemski, L. Viña, G. E. W. Bauer, J. C. Maan, K. Ploog, and G. Weimann, Phys. Rev. B **43**, 14707 (1991).
[20] See Supplemental Material at http://link.aps.org/supplemental/10.1103/PhysRevLett.123.136801, which includes Refs. [1,2,9,16,17,21–37], for description of the experimental details, analysis of an excitonic spectrum in the Kratzer and Rytova-Keldysh potentials, and additional experimental results comprising magnetophotoluminescence and low temperature reflectance contrast spectra of the investigated monolayers.
[21] A. Castellanos-Gomez, M. Buscema, R. Molenaar, V. Singh, L. Janssen, H. S. J. van der Zant, and G. A. Steele, 2D Mater. **1**, 011002 (2014).
[22] X. L. Yang, S. H. Guo, F. T. Chan, K. W. Wong, and W. Y. Ching, Phys. Rev. A **43**, 1186 (1991).

[23] H. A. Bethe and E. M. Salpeter, *Quantum Mechanics of One and Two-Electron Atoms* (Springer-Verlag, Berlin, 1957).

[24] A. V. Stier, N. P. Wilson, K. A. Velizhanin, J. Kono, X. Xu, and S. A. Crooker, Phys. Rev. Lett. **120**, 057405 (2018).

[25] T. C. Berkelbach, M. S. Hybertsen, and D. R. Reichman, Phys. Rev. B **88**, 045318 (2013).

[26] H. Bateman and A. Erdelyi, *Higher Transcendental Functions*, Vol. 1 (McGraw-Hill, New York, 1953).

[27] R. Geick, C. H. Perry, and G. Rupprecht, Phys. Rev. **146**, 543 (1966).

[28] P. Cudazzo, I. V. Tokatly, and A. Rubio, Phys. Rev. B **84**, 085406 (2011).

[29] Y. Li, A. Chernikov, X. Zhang, A. Rigosi, H. M. Hill, A. M. van der Zande, D. A. Chenet, E.-M. Shih, J. Hone, and T. F. Heinz, Phys. Rev. B **90**, 205422 (2014).

[30] A. Arora, M. Koperski, K. Nogajewski, J. Marcus, C. Faugeras, and M. Potemski, Nanoscale **7**, 10421 (2015).

[31] A. Arora, K. Nogajewski, M. Molas, M. Koperski, and M. Potemski, Nanoscale **7**, 20769 (2015).

[32] M. R. Molas, K. Nogajewski, A. O. Slobodeniuk, J. Binder, M. Bartos, and M. Potemski, Nanoscale **9**, 13128 (2017).

[33] C. Robert, M. A. Semina, F. Cadiz, M. Manca, E. Courtade, T. Taniguchi, K. Watanabe, H. Cai, S. Tongay, B. Lassagne, P. Renucci, T. Amand, X. Marie, M. M. Glazov, and B. Urbaszek, Phys. Rev. Mater. **2**, 011001 (2018).

[34] B. Han, C. Robert, E. Courtade, M. Manca, S. Shree, T. Amand, P. Renucci, T. Taniguchi, K. Watanabe, X. Marie, L. E. Golub, M. M. Glazov, and B. Urbaszek, Phys. Rev. X **8**, 031073 (2018).

[35] A. O. Slobodeniuk, Ł. Bala, M. Koperski, M. R. Molas, P. Kossacki, K. Nogajewski, M. Bartos, K. Watanabe, T. Taniguchi, C. Faugeras, and M. Potemski, 2D Mater. **6**, 025026 (2019).

[36] I. C. Gerber, E. Courtade, S. Shree, C. Robert, T. Taniguchi, K. Watanabe, A. Balocchi, P. Renucci, D. Lagarde, X. Marie, and B. Urbaszek, Phys. Rev. B **99**, 035443 (2019).

[37] M. Goryca, J. Li, A. V. Stier, S. A. Crooker, T. Taniguchi, K. Watanabe, E. Courtade, S. Shree, C. Robert, B. Urbaszek, and X. Marie, Nat. Commun. **10**, 4172 (2019).

[38] M. Manca, M. M. Glazov, C. Robert, F. Cadiz, T. Taniguchi, K. Watanabe, E. Courtade, T. Amand, P. Renucci, X. Marie, G. Wang, and B. Urbaszek, Nat. Commun. **8**, 14927 (2017).

[39] C. M. Chow, H. Yu, A. M. Jones, J. Yan, D. G. Mandrus, T. Taniguchi, K. Watanabe, W. Yao, and X. Xu, Nano Lett. **17**, 1194 (2017).

[40] S.-Y. Chen, T. Goldstein, J. Tong, T. Taniguchi, K. Watanabe, and J. Yan, Phys. Rev. Lett. **120**, 046402 (2018).

[41] E. Liu, J. van Baren, T. Taniguchi, K. Watanabe, Y.-C. Chang, and C. H. Lui, Phys. Rev. B **99**, 205420 (2019).

[42] A. Kormányos, G. Burkard, M. Gmitra, J. Fabian, V. Zólyomi, N. D. Drummond, and V. Fal'ko, 2D Mater. **2**, 022001 (2015).

[43] F. Cadiz, E. Courtade, C. Robert, G. Wang, Y. Shen, H. Cai, T. Taniguchi, K. Watanabe, H. Carrere, D. Lagarde, M. Manca, T. Amand, P. Renucci, S. Tongay, X. Marie, and B. Urbaszek, Phys. Rev. X **7**, 021026 (2017).

[44] J. Wierzbowski, J. Klein, F. Sigger, C. Straubinger, M. Kremser, T. Taniguchi, K. Watanabe, U. Wurstbauer, A. W. Holleitner, M. Kaniber, K. Müller, and J. J. Finley, Sci. Rep. **7**, 12383 (2017).

[45] E. Courtade, M. Semina, M. Manca, M. M. Glazov, C. Robert, F. Cadiz, G. Wang, T. Taniguchi, K. Watanabe, M. Pierre, W. Escoffier, E. L. Ivchenko, P. Renucci, X. Marie, T. Amand, and B. Urbaszek, Phys. Rev. B **96**, 085302 (2017).

[46] C. Robert, T. Amand, F. Cadiz, D. Lagarde, E. Courtade, M. Manca, T. Taniguchi, K. Watanabe, B. Urbaszek, and X. Marie, Phys. Rev. B **96**, 155423 (2017).

[47] D. Vaclavkova, J. Wyzula, K. Nogajewski, M. Bartos, A. O. Slobodeniuk, C. Faugeras, M. Potemski, and M. R. Molas, Nanotechnology **29**, 325705 (2018).

[48] P. Nagler, M. V. Ballottin, A. A. Mitioglu, M. V. Durnev, T. Taniguchi, K. Watanabe, A. Chernikov, C. Schüller, M. M. Glazov, P. C. M. Christianen, and T. Korn, Phys. Rev. Lett. **121**, 057402 (2018).

[49] M. Barbone, A. R. P. Montblanch, D. M. Kara, C. Palacios-Berraquero, A. R. Cadore, D. De Fazio, B. Pingault, E. Mostaani, H. Li, B. Chen, K. Watanabe, T. Taniguchi, S. Tongay, G. Wang, A. C. Ferrari, and M. Atatüre, Nat. Commun. **9**, 3721 (2018).

[50] S.-Y. Chen, T. Goldstein, T. Taniguchi, K. Watanabe, and J. Yan, Nat. Commun. **9**, 3717 (2018).

[51] Z. Li, T. Wang, Z. Lu, C. Jin, Y. Chen, Y. Meng, Z. Lian, T. Taniguchi, K. Watanabe, S. Zhang, D. Smirnov, and S.-F. Shi, Nat. Commun. **9**, 3719 (2018).

[52] M. R. Molas, A. O. Slobodeniuk, T. Kazimierczuk, K. Nogajewski, M. Bartos, P. Kapuściński, K. Oreszczuk, K. Watanabe, T. Taniguchi, C. Faugeras, P. Kossacki, D. M. Basko, and M. Potemski, Phys. Rev. Lett. **123**, 096803 (2019).

[53] E. Liu, J. van Baren, Z. Lu, M. M. Altaiary, T. Taniguchi, K. Watanabe, D. Smirnov, and C. H. Lui, Phys. Rev. Lett. **123**, 027401 (2019).